Mon. Not. R. Astron. Soc. **289,** 525–534 (1997)

Steep-spectrum radio cores in high-redshift galaxies

R. M. Athreya,[1]★ V. K. Kapahi,[1] P. J. McCarthy[2] and W. van Breugel[3]
[1]*National Centre for Radio Astrophysics (TIFR), PO Bag 3, Ganeshkhind, Pune 411 007, India*
[2]*Observatories of the Carnegie Institution of Washington, 813 Santa Barbara Street, Pasadena, CA 91107, USA*
[3]*IGPP/Lawrence Livermore National Laboratories, PO Box 808, Livermore, CA 94550, USA*

Accepted 1997 March 5. Received 1997 March 5; in original form 1996 January 24

ABSTRACT

We have made high-resolution radio images, using the Very Large Array (VLA), of a sample of radio galaxies at $z > 2$ selected from the MRC/1 Jy complete sample. These are also the first detailed observations of radio galaxies at the high rest-frame frequencies of 15–30 GHz. Compact (<0.2 arcsec) cores at the mJy and sub-mJy level were detected in most of the objects, coincident with the optical galaxies. In sharp contrast to the flat spectra of radio cores in galaxies at low redshift, we find that most of the cores at high redshift have a steep spectral index ($\alpha > 0.5$) between 4.7 and 8.3 GHz (observed). We identify this steepening with the optically thin part of a synchrotron self-absorbed spectrum at frequencies above the turnover. Both core- and lobe-dominated quasars have also been reported to show such a turnover from flat to steep spectra but at much higher observed frequencies. We suggest that the cores in galaxies and quasars are intrinsically similar (in the rest frame of the emitting plasma) and that the observed differences can be explained in terms of Doppler shifting by different amounts in quasar and galaxy cores. This model is consistent with the unification scheme for radio galaxies and quasars.

Using the theory of synchrotron self-absorption we estimate sizes of $\sim$ 1 pc, magnetic fields of $\sim$1 G and electron densities of $\sim$1000 cm^{-3} for the cores of both quasars and radio galaxies. The similar values are perhaps an indication of similar physical processes and parameters in their cores. The spectrum at turnover provides information on scales much smaller than the telescope resolution. It is therefore a useful tool for probing the cores of galaxies which are usually too weak for very long-baseline interferometry studies.

Key words: galaxies: nuclei – radio continuum: galaxies.

1 INTRODUCTION

Radio and optical observations being carried out for a complete sample of 558 radio sources from the Molonglo Reference Catalogue (McCarthy et al. 1991, 1996; Kapahi et al., in preparation) have already led to the discovery of about 20 radio galaxies at redshifts >2.0. In addition to their many interesting properties, the radio sources in these galaxies are useful as probes of the environment at high redshifts; it is hoped that studies of these objects will considerably improve our understanding of the earliest epochs of galaxy formation. As a follow-up of our initial survey, we have undertaken a detailed radio study of 15 of the high-redshift radio galaxies (HRRGs) from our sample (Athreya 1996). Studies of HRRGs have so far focused mainly on their optical and infrared properties. Only two radio galaxies, 4C 41.17 ($z = 3.8$) and 0902+343 ($z = 3.4$), have been studied in some detail in the radio so far (Carilli, Owen & Harris 1994; Carilli 1995). Our radio observations of the 15 galaxies provide the first extensive data set with which to study the general properties of the radio galaxy population at $z > 2.0$. Results from this study on various aspects including morphology, energetics, polarization, etc. will be discussed in subsequent papers.

We present in this paper a discussion of the observed properties of the radio cores of HRRGs; this is also the first time that the cores of radio galaxies have been studied at high rest-frame frequencies of 15–30 GHz. In contrast to the flat-spectrum radio cores found at lower redshifts (and hence lower rest-frame frequencies) we find that a large fraction of the cores in HRRGs have a steep radio spectrum.

The canonical powerful radio source associated with a quasar or a radio galaxy consists of a parsec-scale radio core coincident with the optical galaxy and extended emission ranging from a few kpc to over a Mpc in size on either side of the core. In the extensively studied radio region of 100 MHz to 10 GHz, the emission from the compact core almost always has a flat or inverted spectrum ($-1.0 \lesssim \alpha < 0.5; S_\nu \sim \nu^{-\alpha}$). The extended emission on the other

★E-mail: ramana@gmrt.ernet.in

hand has a steep spectral index of $\alpha \sim 0.7-1.0$ and occasionally even higher. Sources dominated by the extended emission are found in both radio galaxies and quasars. The flat-spectrum cores in such sources typically contribute a few per cent of the total flux (galaxies generally having much weaker cores than quasars). Sources dominated by the core emission are almost always quasars and BL Lac objects. Most studies of radio cores have therefore focused on quasar cores, particularly those in flat-spectrum core-dominated quasars (CDQs) which have been found to exhibit many remarkable properties such as superluminal motion and rapid variability (see e.g. Miley 1980 and Kellermann & Pauliny-Toth 1981 for reviews on radio sources).

The spectra of the cores of CDQs are known to remain remarkably flat over two or three decades of frequency between ~100 MHz and ~100 GHz (Kellermann & Pauliny-Toth 1969; Cotton et al. 1980). This is believed to be a result of superposition of spectra of several components which undergo synchrotron self-absorption (SSA) at different frequencies. The emission below the SSA turnover frequency is optically thick and has an inverted spectrum ($\alpha < 0$); the emission is optically thin at frequencies above the turnover and has the usual steep spectrum (e.g. Pacholczyk 1970; Moffet 1975).

The spectra of CDQs become optically thin and steepen only in the mm and submm wavelength region (Impey & Neugebauer 1988; Sanders et al. 1989; Gear et al. 1994). This steepening can be related to the size of the smallest emission region. Lack of resolution and limited sensitivity of the mm-wave telescopes makes the study of weak cores of extended sources (including lobe-dominated quasars) impractical if not impossible. Only in the last few years have the cores of a few extended quasars been studied at mm wavelengths (Antonucci, Barvainis & Alloin 1990; Gopal-Krishna & Steppe 1990). The objects had to be chosen with care to ensure that the core measurements were not contaminated by the extended emission. It has not been possible to study the cores of radio galaxies at these wavelengths although some observations of the total radio emission have been made (e.g. Knapp, Bies & van Gorkom 1990). Radio galaxies at high redshift offer us the possibility of studying the cores at fairly high rest-frame frequencies.

We discuss in this paper the steep spectra exhibited by the cores of HRRGs at rest-frame frequencies of 15–30 GHz. This is compared with a similar steepening shown by quasars at even higher frequencies. We identify the steep spectra of the cores with the optically thin region of a synchrotron self-absorbed spectrum. The difference between the quasar and galaxy cores can be explained in terms of differential Doppler shifting of intrinsically similar spectra. We discuss the implication of these results for the unification schemes of radio galaxies and quasars and for the spectral energy distribution of radio sources from the radio to the far-infrared. From the observed spectra and the theory of synchrotron self-absorption we derive physical parameters of the cores of radio sources including the size, the magnetic field and the number density of electrons. This has hitherto not been possible for the weak cores of distant radio galaxies.

2 OBSERVATIONS AND RESULTS

The details of the observations and the radio images are being presented in Athreya et al. (in preparation; see Athreya 1996). In brief, multifrequency polarimetric observations of 15 galaxies at $z > 2$ were made using the Very Large Array, USA. The details of the observations relevant to this paper are listed in Table 1.

Table 1. VLA observations of high-redshift radio galaxy cores. The bandwidth is 50 GHz at all frequencies. The mean frequencies are given within angular brackets.

Frequencies GHz	Array	Resoln. arcsec	Proj. No.	Date
4.5351,4.8851 ⟨4.71⟩	A	0.4–0.9	AC374	18 Mar 94
8.0851,8.3351 ⟨8.21⟩	A	0.2–0.4	AC374	18 Mar 94
8.4149,8.4649 ⟨8.44⟩	BnA	0.5–0.7	AA155	14 Feb 93

The data were analysed using the AIPS package distributed by the NRAO and the standard procedure detailed in the AIPS manual. The analysis included a flux density calibration using observations of 3C 286 and 3C 48 and the scale of Baars et al. (1977), including the corrections recently incorporated by Perley in the AIPS package. It was followed by phase calibration and 3–4 rounds of self-calibration (phase only) to improve the quality of the images. The typical rms noise in the final images is 0.05–0.1 mJy beam^{-1}.

A compact radio component coincident with the optical galaxy is usually identified as the radio core. In almost all the radio sources known so far, the core, and only the core, has a flat spectrum; consequently the spectrum has become the prime criterion for identifying the core. Since all the components in most of our sources have a steep spectrum, we have identified the cores by their compact size and positional coincidence with the optical galaxy. The coordinates of the associated optical galaxy were determined from stars in the CCD field of the object, the positions of which were measured on digitized sky survey plates. We expect an rms error of ~1 arcsec between the radio and optical positions owing to several factors including the small number of reference stars in each field (typically 1–3), the faintness of the extended optical object and the discrepancy between the radio and optical reference frames in the poorly sampled southern hemisphere [see McCarthy et al. (1996) and Athreya (1996) for a more detailed discussion of the identification of the optical counterpart and the radio core].

Of the 15 radio galaxies, only one was unresolved at all frequencies. Cores were identified in 12 of the remaining 14 extended sources. The flux densities and spectral indices of HRRG cores are presented in Table 2 (see also Fig. 1). Considering the small interval between the frequencies and the consequent large error in the spectral index, particular care was taken in estimating the flux densities of the faint cores and the errors on them.

The 4.71- and 8.21-GHz images were obtained from snapshots of a few min duration at two different hour angles and have some amount of spurious structures at the ~0.15 mJy beam^{-1} level. This can result in a substantial contamination of cores weaker than 0.5 mJy beam^{-1} particularly in sources in which the core and the lobes are not well separated. The 8.44-GHz images were somewhat better as they were from longer observations at about 3–4 hour angles. The agreement between the fluxes measured at 8.21 and 8.44 GHz, obtained from observations separated by a year, indicated not only the absence of flux variability over the period but also the fidelity of the images. Since the resolution at 8.21 GHz was higher than that at 8.44 GHz by a factor of 2, the agreement between the flux densities also suggested that the core identifications were indeed compact with very little contribution from a 'halo', if any. The flux densities were measured using the IMFIT program in AIPS which fits a Gaussian to the intensity distribution. The deconvolved sizes of the stronger cores were all consistent with them being 'point sources' with deviations only at the level of a few per cent of their peak flux. The

Table 2. Radio core spectra of galaxies at $z > 2$.

Source	$S_{4.71\,GHz}$	$S_{4.86\,GHz}$	$S_{8.21\,GHz}$	$S_{8.44\,GHz}$	α_s	α_{peak}
0015-229 c1	1.13 ± 0.10	-	0.67 ± 0.07	–	0.94 ± 0.26	(0.4–0.82) ± 0.28
0015-229 c2	2.9–3.8 ± 0.19	-	1.47 ± 0.10	–	(1.22–1.71) ± 0.18	(0.95–1.1) ± 0.17
0140-257	0.71 ± 0.09	-	0.37 ± 0.07	0.43 ± 0.07	1.00 ± 0.38	1.20 ± 0.39
0156-252	10.5 ± 0.53	-	6.67 ± 0.35	6.80 ± 0.36	0.78 ± 0.12	0.70 ± 0.12
0316-257	0.36 ± 0.13	-	0.28 ± 0.06	0.26 ± 0.03	0.51 ± 0.56	(0.47–0.84) ± 0.54
0349-211	–	7.2 ± 0.4	–	12.20 ± 0.61	−0.96 ± 0.14	–
0406-244	2.36 ± 0.21	-	1.48 ± 0.09	1.51 ± 0.14	0.80 ± 0.18	0.79 ± 0.16
1106-258	0.69 ± 0.06	-	0.26 ± 0.08	–	1.76 ± 0.43	1.80 ± 0.50
1138-252	5.10 ± 0.32	-	3.30 ± 0.22	2.90 ± 0.25	0.88 ± 0.16	(0.62–0.86) ± 0.14
1324-264	$\lesssim$ 0.95 ± 0.09	-	0.95 ± 0.07	–	$\lesssim$ 0.00 ± 0.22	–
2025-218	0.65–0.85 ± 0.10	-	0.36 ± 0.09	–	(1.06–1.55) ± 0.54	1.10 ± 0.48
2036-254	0.43 ± 0.09	-	0.28 ± 0.07	–	0.77 ± 0.60	0.10 ± 0.52
2104-242	–	$\lesssim$ 0.70	–	0.64 ± 0.09	$\lesssim$ 0.16 ± 0.47	–

Notes:
(i) The columns list the source name, flux density in mJy (S with the frequency in subscript), the spectral index from the flux densities listed (α_s) and the spectral index from the peak fluxes in the super-resolved images with identical resolution at 4.71 and 8.44 GHz (α_{peak}).
(ii) A hyphen (-) indicates lack of observations.
(iii) The values for both the core candidates in 0015-229 are listed; c2 is more likely to be the radio core.
(iv) The extremities of the range listed at 4.71 GHz (and consequently the α_s also) in 0015-229 and 2025-218 are the peak flux from the super-resolved image (lower value) and the flux density (upper value) obtained from IMFIT. The lower value is likely to be more appropriate for the flux density as well since the core appears to be located on a plateau which may be spurious.
(v) Insufficient resolution in some images resulted in the core being barely resolved from the lobe at one frequency in 1324-264 and 2104-242; the upper limits listed are due to the difficulty in estimating the flux and not due to non-detection of the core.
(vi) α_{peak} was not calculated for 0349-211 and 2104-242 since the images at the two frequencies were of very different resolutions. In 1324-264, the core was not sufficiently distinct from the lobe at 4.71 GHz.
(vii) The extremities of the range listed for α_{peak} in 0015-229 and 0316-257 correspond to the peak fluxes obtained after subtracting (lower value) and without subtracting (higher value) the plateau in the 1D slices across the cores in the 4.71-GHz images.
(viii) Super-resolution images indicate that the peak flux of the core in 1138-262 is 3.69±0.2 mJy (4.71 GHz) and 2.23±0.13 mJy (8.21 GHz) which is considerably less than the flux densities obtained from IMFIT.
(ix) The 4.86-GHz values are from Kapahi et al. (in preparation).

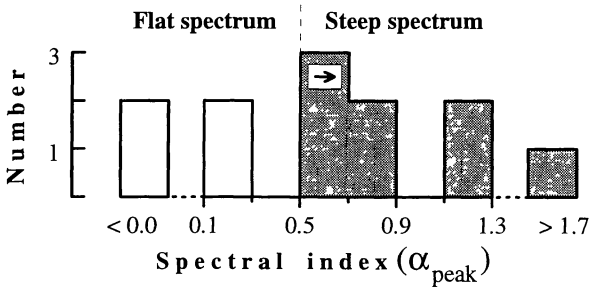

Figure 1. Histogram of core spectral indices of radio galaxies at $z > 2$. The values plotted are listed in Table 2. α_s has been used for sources without α_{peak} values.

weaker cores deviated from a point source structure at a higher level of up to 20 per cent of their peak flux; however this is to be expected since 20 per cent of their peak is equivalent to 1–1.5σ of the images.

We also made super-resolved images at 4.71 and 8.44 GHz (with a few at 8.21 GHz) with *identical* resolutions of ~0.3–0.5 arcsec (i.e. 30–50 per cent super-resolution) at both frequencies in order to minimize lobe contamination of core fluxes (the contamination, which is likely to be more at 4.71 GHz as a result of the very steep spectra of radio lobes in high-redshift galaxies, may 'steepen' the core spectral index). However, an examination of the *clean components* in the super-resolved images showed that the cleaned flux density was confined to a few pixels (2–5) at the location of the peak (beam size ~20–25 pixel) indicating very little contamination of the core flux density owing to extended components. This also confirmed the compact nature of the core identifications. It should be noted here that super-resolving faint components to bring out their structure is fraught with pitfalls; however, the super-resolution attempted here was not for delineating their fine structure but only to check that they did not have any.

The peak flux should be numerically identical to the flux density of a point source. It is also likely to be a better estimate of the total flux density since it is less contaminated by adjacent noise peaks. So we also calculated the core spectral indices from their peak flux values in the super-resolved images at 4.71 and 8.44 GHz. The peak values were obtained from Gaussian fits to 1D slices across the cores (using SLICE and SLFIT). The 1D slices were taken along the core–hotspot axis since contamination of the core owing to the tail of the lobe emission or a faint jet is more probable along the radio axis. These α_{peak} values are also listed in Table 2 and are likely to be more accurate than the spectral indices calculated from flux densities for the reasons described above.

All the radio images are being published in Athreya et al. (in preparation). Brief notes of the quality of the radio images have been given below. The radio cores of 0156-252, 0349-211, 0406-244, 1138-252 and 1324-264 were all $\gtrsim$1 mJy even in the 8-GHz bands (rms noise < 10 per cent of their flux in all cases). Further, the cores were many times stronger than the contiguous jets and presented little difficulty in the calculation of spectral indices.

The worst case was in 1324-264 where the resolution did not permit the separation of the core and jet in the 4.71-GHz image. Similarly, while the 8-GHz observations were able to completely separate the core from the lobes in 2104-242, the insufficient resolution at 4.8 GHz provided only an upper limit to the flux density. In the case of 0015-229, 0316-257 and 2025-218, the 1D slices of the 4.71-GHz images showed that the cores were sitting on a 'pedestal' of ~0.1–0.2 mJy beam^{-1} which extended all along the slice. It is not clear what fraction of the pedestal was actually contributed by the core itself and what fraction was spurious (or arising from the tail of the lobe). The spectral indices of these sources were calculated both by adding the flux of the pedestal to the core and otherwise. There are two possible candidates for the core in 0015-209, one of which has a marginally steep spectrum while the other has a considerably steep spectrum. The radio cores of 0140-257, 0316-257, 1106-258, 2025-218 and 2036-254 were fainter and consequently contaminated by noise in the images. All quoted errors are quadratic sums of the rms noise and the error from the flux density fitting programs (IMFIT and SLFIT). Additional notes on some sources are given below Table 2.

A surprisingly large fraction of the sources have steep-spectrum cores. Of the 12 cores, eight have a steep spectrum ($\alpha > 0.5$), three are flat ($0 < \alpha < 0.5$) and one is inverted ($\alpha = -0.98$). This result is unlikely to be a statistical artefact in spite of the considerable errors on some α values and the small number of sources involved, as discussed below.

Going by the incidence (or lack of it) of steep-spectrum radio cores in radio galaxies at lower redshift, one would not have expected to see any such object in a sample of 12 HRRGs. That eight of the galaxies have steep-spectrum cores makes it very unlikely that the result is a statistical artefact. Although the large errors in some individual core spectral indices could have considerably modified the shape of the distribution of the core spectral indices (Fig. 1) they are not large enough to vitiate this result. It must also be noted that the errors are random in nature and are as likely to have flattened the core spectral indices as steepened them. Finally, four of the six strong cores (>1 mJy at 8 GHz; with high signal-to-noise ratio) in the sample have steep spectra.

Several steep-spectrum cores were reported earlier by Bridle & Fomalont (1978) in a sample of low-redshift radio galaxies. Their observations were, however, made with angular resolutions of several arcsec. They inferred sizes of 2–6 kpc for the steep-spectrum cores while the flat-spectrum cores were unresolved even at the highest resolution and were expected to be much smaller than a kpc. However, subsequent observations showed that the steep spectrum, in several cases, was a result of a 'halo' of extended emission around a weaker flat-spectrum compact core (Saikia, Kulkarni & Porcas 1986). Other 'steep-spectrum cores', like in 3C 236 and 3C 293, actually turned out to be several compact steep-spectrum knots strung across a kpc in which a much weaker flat-spectrum component was eventually found (e.g. Bridle, Fomalont & Cornwell 1981; Barthel et al. 1985). The cores of the radio galaxies in our study have been observed with a resolution of 0.2 arcsec (linear size of $0.7\,h^{-1}$ kpc with $H_0 = 100\,h\,\mathrm{km\,s^{-1}\,Mpc^{-1}}$, $\Omega_0 = 1$) and are unresolved even at that scale. The images indicate that they are likely to be smaller than the telescope resolution by factors of at least 2–3 which makes them smaller than a kpc in size.

With the present resolution we are unable to rule out the possibility of parsec-scale steep-spectrum jets and a much weaker flat-spectrum core component. Only milliarcsec VLBI at 1–20 GHz will be able to tackle this question. However, it may be noted that observations of radio sources at $0.5 < z < 1.5$, at similar frequencies and angular resolutions, have not resulted in the detection of steep-spectrum cores. The fairly flat relationship between angular size distance and redshift for $0.5 < z < 3$ for most values of non-zero Ω_0 suggests that the lack of linear resolution is unlikely to have resulted in steep-spectrum cores.

We believe that these sub-kpc sized components, though with steep spectra, are the *true* radio cores rather than surrounding haloes or knots in the jets. The core spectral index showed no significant correlation between other source parameters like redshift, total luminosity, core luminosity, core fraction, total spectral index, etc.

3 DISCUSSION

3.1 Core spectra

This study of radio cores differs from others in two ways – the radio sources are at very high redshifts and are being studied at high rest-frame frequencies. Interferometry at frequencies above 15 GHz has been confined to VLBI studies which require strong and compact sources. This has limited high-resolution (subarcs to tens of μ arcsec) studies at these frequencies to core-dominated quasars. Subarcsec studies of the radio cores in this sample at 20–30 GHz in the rest frame have been possible with the existing facilities only because of the high redshift of the sources. The HRRG cores in this study have only been observed at high rest-frame frequencies (> 15 GHz) while low-redshift radio galaxy cores have hitherto been studied only at lower rest-frame frequencies ($\lesssim$15 GHz). This suggests two lines of enquiry for an explanation of the steep spectra in the cores of HRRGs – a *frequency* effect and a *redshift* effect. Until radio galaxy cores at both high and low redshifts are studied with sufficient resolution and sensitivity at both low and high rest-frame frequencies, it will not be possible to unambiguously rule out one or the other explanation. However, the data from quasar cores as well as the well established theory of synchrotron emission offer some clues in this matter.

The *redshift* hypothesis is that the cores of HRRGs have steep spectra over the entire range of radio frequencies normally observed (0.1–100 GHz) while the spectra of low-redshift radio cores are flat in the same range. There are, as of now, no compelling reasons, either observational or theoretical, for adopting such a hypothesis. One possible explanation could be that the putative higher density of the ambient gas disrupts the jet to some extent resulting in a halo of steep-spectrum emission around a flat-spectrum jet. Though this cannot be ruled out as of now, we believe that the explanation lies in the higher rest-frame frequency at which the cores have been studied.

The spectral indices of the HRRG cores have been calculated at ~20–30 GHz in the cosmological rest-frame (crf) of the source. The steep spectra can be understood if the smallest components in the cores of radio galaxies have SSA turnovers at $\nu_{\mathrm{ssa}} \approx 5$ GHz in the crf. Previous studies of radio galaxy cores have gone up to 10–15 GHz (sources at $z \gtrsim 1$) in the crf but have not reported cores steeper than $\alpha = 0.5$. The region of 5–20 GHz is probably the transition zone in which optical depth varies from ~1.0 to $\ll$1. Other studies have shown that quasar cores also turnover from flat to steep spectra though at considerably higher crf frequencies. We compare the steepening in quasar cores with that observed in HRRGs and explain the difference in terms of intrinsically similar cores modified by relativistic aberration (i.e. flux boosting as well as Doppler shifting).

3.1.1 *Core spectra of quasars*

Core-dominated quasars

The flat spectra of the cores of blazars have been known to steepen at rest frequencies of a few 100 GHz (Jones et al. 1981; Impey & Neugebauer 1988; Brown et al. 1989; Sanders et al. 1989). Gear et al. (1994) have presented quasi-simultaneous flux density measurements of a sample of 22 BL Lac objects ($z < 1.0$) and 22 CDQs ($z < 1.5$). Their multifrequency dataset (10 frequencies between 5 and 375 GHz) is ideal for studying the shapes of the radio spectra over a wide frequency range in the source crf. Their observations of blazars fill up the lacuna in previous studies in the crucial mm region. Using their data, we have constructed the 2-point spectral index distribution for the sources at 6.3, 10.6, 17.5, 28.5, 46.8, 76.7, 116, 193, 306, 501 and 823 GHz in the crf (these frequencies are the geometric means of those used to calculate the 2-point spectral indices, the ratio of neighbouring frequencies being ~1.65). Spectral index distributions were constructed for the entire sample of CDQs as well as for high- and low-redshift objects separately, the division being arbitrary ($z = 0.7$) and chosen to provide equal numbers in each.

The crf spectral index distributions are plotted in Fig. 2; quasar (and BL Lac – see Section 3.3 for a discussion on BL Lac spectra) distributions are plotted in the first panel (Fig. 2a) while high- and low-redshift quasars in the second (Fig. 2b). The median spectral index and the 1σ of the distribution (using binomial statistics) have been plotted at each frequency.

The quasar distributions (Figs 2a,b) show a marked change in the median value between 76.7 and 193 GHz (hereafter referred to as the break frequency range or simply the break). The median spectral index values and much of the distribution at frequencies below the break are flatter than 0.5. All frequencies above the break have the median values as well as much of the distribution steeper than 0.5. Some simple numerical calculations showed that the difference in frequency between $\alpha = 0.0$ and 0.5 is a factor of ~3. The mean spectral index appears to be 0.5 at ~150 indicating that the *typical* turnover is at ~50 GHz in the rest frame. However it must be noted that the distribution in the turnover frequency is likely to be fairly broad and the turnover in individual sources could differ from the typical value by as much as a factor of 2.

This is true for both the redshift classes. The spectral indices beyond the break do not appear to steepen (within errors) towards higher frequencies. However the higher redshift objects appear to be consistently steeper. Averaging all the spectral indices above the break accentuates this difference (Table 3). The spectral index distributions are fairly broad at every frequency and the high-redshift sample is steeper at 90 per cent significance level (Kolmogorov–Smirnov 1-tailed test) though the difference in the *mean spectral indices* between the high- and low-redshift quasars is significant at the >99 per cent level.

Lobe-dominated quasars (LDQs)

The cores of a sample of low-redshift LDQs were observed in the mm region by Antonucci et al. (1990) and Gopal-Krishna & Steppe (1990) to determine the thermal and non-thermal contributions to the far-infrared emission of these sources. These sources show a turnover in their spectrum at ~ 20 GHz in the crf.

Lonsdale, Barthel & Miley (1993) noted that 'an inspection of the contour maps revealed many steep-spectrum cores' in LDQs at $z > 1.5$ between 4.8 and 15 GHz (observed frame). However the lack of spectral index values for the sources in their paper precludes a quantitative comparison of the incidence of steep-spectrum cores in radio galaxies and quasars at high redshifts.

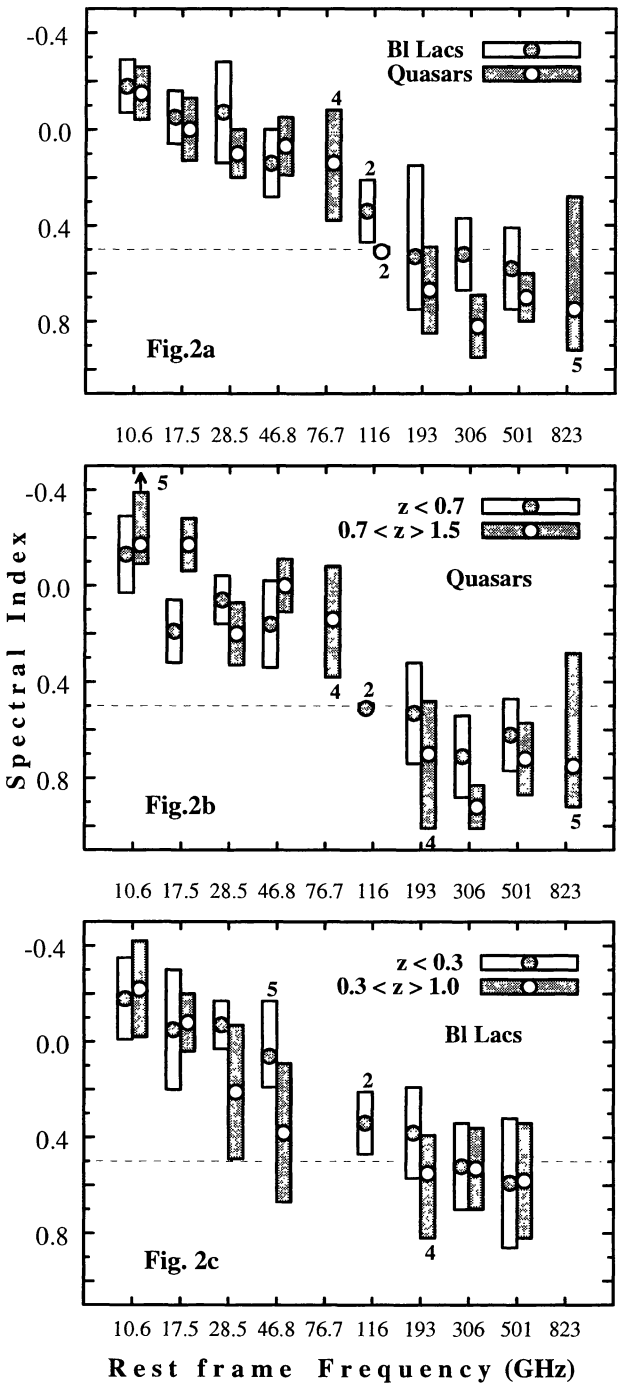

Figure 2. Cosmological rest-frame spectral index distributions of core-dominated quasars and BL Lacs constructed using the data from Gear et al. (1994). The circles in the vertical bars represent the median spectral index while the bars represent the 1σ of the distribution at each frequency. The numbers of data points in frequency bins with five points or fewer have been indicated against the respective bars. The top panel compares BL Lacs and quasars, the middle one compares quasars at low and high redshifts while the bottom panel shows BL Lacs at low and high redshifts.

3.1.2 *Model for the core spectrum*

We emphasize here the difference between the *cosmological rest*

Table 3. Mean spectral indices of blazars at frequencies (cosmological rest frame) above the synchrotron turnover.

Sources		N	$\langle\alpha\rangle^a_{\nu>150\,\mathrm{GHz}}$	$\langle\alpha\rangle^b_{\nu>150\,\mathrm{GHz}}$
CD quasar	$z<0.7$	44	0.64 ± 0.02	0.67 ± 0.02
	$0.7<z<1.5$	33	0.75 ± 0.02	0.75 ± 0.02
BL Lacs	$z<0.7$	54	0.46 ± 0.02	0.48 ± 0.02
	$z<0.3$	35	0.43 ± 0.03	0.46 ± 0.03
	$0.3<z<1.0$	30	0.54 ± 0.03	0.56 ± 0.03
			$\langle\alpha\rangle^a_{\nu>300\,\mathrm{GHz}}$	$\langle\alpha\rangle^b_{\nu>300\,\mathrm{GHz}}$
BL Lacs	$z<0.3$	23	0.50 ± 0.03	0.51 ± 0.04
	$0.3<z<1.0$	26	0.54 ± 0.04	0.54 ± 0.04

Notes: The values have been calculated from the data in Gear et al. (1994). The 2-point spectral indices of all the sources at all the frequencies greater than the turnover have been averaged (see Fig. 2). $\langle\alpha\rangle^a$ is the error weighted mean of the entire distribution while $\langle\alpha\rangle^b$ is the error weighted mean after excluding 5 extreme points on each side of the distribution (to check the effect of extreme points on the mean value). N is the number of 2-point spectral index values obtained from adjacent pairs of frequencies above 150 GHz as discussed earlier; each source contributes spectral index values at 2–4 frequency pairs.

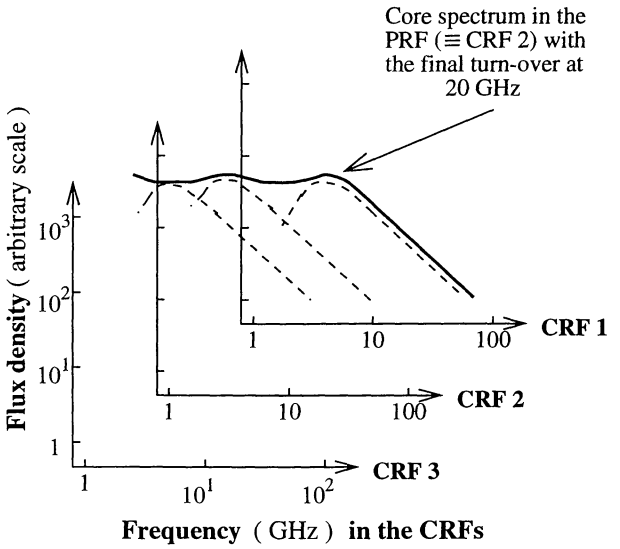

Figure 3. The model core spectrum in the cosmological and plasma rest frames. The core spectrum is indicated by the thick solid line and is the superposition of the spectra of individual components (thin dashed line) which undergo synchrotron self-absorption at different frequencies. The three cosmological rest frames, CRFs 1, 2 and 3, are Doppler shifted by factors of 0.2, 1 and 5, respectively, with respect to the plasma rest frame (i.e. CRF 2 ≡ PRF). For a Lorentz factor $\gamma = 10$, the Doppler factors correspond to $\theta = 60°$, 25° and 10° respectively. These are consistent with the typical viewing angles for radio galaxies, lobe-dominated and core-dominated quasars, respectively, in Barthel's scheme for galaxy–quasar unification.

frame of the source (crf) and the *rest frame of the emitting plasma* in the core (prf); the plasma is moving at relativistic speeds in the crf. The relationship between the frequencies as measured in the crf and the prf is given by $\nu_{\mathrm{crf}} = \nu_{\mathrm{prf}}\Gamma$, where the Doppler factor $\Gamma = [\gamma(1-\beta\cos\theta)]^{-1}$ (see Fig. 3).

In the unified scheme for radio galaxies and quasars (Barthel 1989) the only difference between the classes is that quasar cores are viewed at angles close to the jet axis while galaxies are viewed nearly perpendicular to the jet axis. The flux boosting in quasar cores is accompanied by a blueshift of the spectrum while the dimming of galaxy cores is accompanied by a redshift. The difference between the ν_{ssa} (crf) of quasar and radio galaxy cores can be understood in terms of intrinsically similar spectra in the prf Doppler shifted by different amounts due to relativistic aberration.

Based on the above observations we suggest that core spectra of galaxies and quasars are flat at frequencies below $\nu_{\mathrm{ssa}} \approx 20$ GHz in the prf and steepen to about $\alpha \approx 0.7$ above the turnover. We emphasize here once again that the distribution of the turnover frequencies in radio cores is fairly broad and could extend on either side of this typical value by a factor of 2–3. In the crf, this ν_{ssa} is Doppler shifted by a factor of 3–5 (i.e. a blueshift) in CDQs (Fig. 2), by ~1 in LDQs (Antonucci et al. 1990; Gopal-Krishna & Steppe 1990) and by ~0.2 (a redshift) in radio galaxies (our sample). These values correspond typically to a viewing angle of ~10° for CDQs, ~25° for LDQs and ~60° for galaxies using $\gamma \sim 10$ and are consistent with Barthel's scheme. This model has been shown schematically in Fig. 3.

Impey & Neugebauer (1988) have reported a mean turnover frequency of ~200 GHz (crf) for blazars, which is much higher than the value we derive from the data of Gear et al. (1994). The crucial difference between the two studies is the lack of data between 100 and 400 GHz in the former (they were studying the overall radio–infrared–optical continuum) while the latter concentrated on filling the mm/submm gap in the radio spectra. The higher frequency resolution of Gear et al. shows a turnover at ~100 GHz (discussed in this paper), following which the spectrum rises again towards higher frequencies and turns over once more at ~1000 GHz. This second turnover is believed to be due to emission from (non-relativistic) hot dust around the nucleus (see also Bregman 1990 and references therein). The spectra in Impey & Neugebauer, owing to the lack of mm/submm fluxes, do not show the discontinuity between the radio and the infrared and hence were fitted by smooth curves with only one turnover at a frequency in between the separate turnovers in the radio and the infrared.

While the observed flux from CDQs at wavelengths longer than 100 μm is dominated by the Doppler boosted and blueshifted synchrotron emission, the dust emission at ~100 μm is likely to be much more than the unboosted synchrotron emission in the plasma rest frame. The rest-frame contributions from the various processes in the spectral region of 1 cm–100 μm in the host galaxy nuclei would be best studied in LDQs since their core spectra (with Doppler factors of ~1) are the least modified by Doppler boosting.

While discussing the flatter core spectra of BL Lacs compared to CDQs, Gear et al. (1994) considered and rejected the possibility that the difference was as result of different angles made by their jets to the line of sight. However, as shown in this paper, the differences in the observed radio core spectra of quasars and radio galaxies can be explained by relativistic beaming and different jet viewing angles for the two classes.

3.1.3 Steep-spectrum cores in a sample of randomly oriented sources

Based on the above model we derive here the fraction of steep-spectrum cores that one expects to see in a complete sample of randomly oriented sources.

Let $\nu^{\mathrm{st}}_{\mathrm{prf}}$ and $\nu^{\mathrm{st}}_{\mathrm{crf}}$ be the frequencies beyond which the spectral index of the core is steeper than 0.5 in the prf and crf respectively ($\nu^{\mathrm{st}}_{\mathrm{crf}} = \nu^{\mathrm{st}}_{\mathrm{prf}}\Gamma$). Let ν_{crf} be the CRF frequency at which the core

spectral index has been calculated for a complete sample of randomly oriented radio sources. Sources which satisfy $\nu_{\rm crf} > \nu^{\rm st}_{\rm crf} (\equiv \nu^{\rm st}_{\rm prf}\ \Gamma)$ will have a steep-spectrum core. The fraction of sources with steep cores is given by the probability $P(\Gamma < \Gamma^{\rm st})$ with $\Gamma^{\rm st} = (\nu_{\rm crf}/\nu^{\rm st}_{\rm prf})$. Using $({\rm d}P/{\rm d}\theta) = \sin\theta$ and the relationship between θ and Γ, we get

$$P(\Gamma < \Gamma^{\rm st}) = \left(\frac{1}{\beta}\right)\left(1 - \frac{1}{\gamma\Gamma^{\rm st}}\right). \quad (1)$$

Using $\nu_{\rm crf} = 20$ GHz and $\nu^{\rm st}_{\rm crf} = 75$ GHz, we get $\Gamma^{\rm st} = 0.267$. This corresponds to a steep-spectrum core fraction of 0.63 in a randomly oriented sample of sources (for $\gamma = 10$), i.e. all sources with $\theta > 51°$. It is to be noted that for a single value of $\nu^{\rm st}_{\rm prf}$ and γ, all sources greater than a critical angle (between the jet and the line of sight) will have steep spectra. In the context of Barthel's unified scheme for galaxies and quasars, steep-spectrum quasar cores will begin to appear only at frequencies above which all galaxy cores are steep. However, in case of a spread in $\nu^{\rm st}_{\rm prf}$ and γ values, as appears more likely, a few steep quasar cores will be encountered even before all galaxy cores have steepened. This is borne out by the incidence of steep-spectrum cores in high-redshift LDQs reported by Lonsdale et al. (1993). This is also indicated by some high-redshift quasars with D2 structure (extended emission on one side of the radio core only) in our complete Molonglo sample which have a dominant core and yet have a steep spectrum (Kapahi et al., in preparation).

3.2 Core parameters

Several parameters including the linear size, magnetic field and the electron density of the emitting component can be calculated from the observed turnover using the theory of synchrotron self-absorption (see Appendix). The popular paradigm of the central engine of a radio source consists of a super-massive black hole ($\sim 10^9$ $M_\odot$) powered by an accretion disc which gives rise to a pair of relativistic jets. The smallest core component would be the base of the jet from where the radio emission first arises as the the jet propagates outwards. The parameters estimated using the spectrum beyond the final turnover should pertain to this 'smallest' component in the core (hereafter the core refers to this μarcsec base of the jet and not the usual arcsec core).

The observed spectral parameters and the derived values for the cores have been tabulated in Tables 4 and 5 respectively. The derived values are similar for the radio galaxies and quasars except for the electron density in some LDQs.

The main uncertainty in these values, especially the electron density, stems from the (unknown) Doppler factors of radio galaxies and LD quasars. The parameters have been derived for different Lorentz γ values using Barthel's model for the viewing angle of galaxies and quasars.

Apart from the Doppler factors, several parameters like the turnover frequency and the spectral index at frequencies above the turnover are not well determined for individual sources (changing α from 0.6 to 1.1 makes a difference of an order of magnitude in electron density; in fact, the two sources with the most discrepant values for the number density have the highest spectral indices). Further, many simplifying assumptions have gone into the equations used in estimating the parameters (see Appendix) which may not be strictly valid especially in the case of strongly relativistic jets. Another point to be remembered is that in case of a distribution of γ values in the cores, as is likely, telescope sensitivity limits will select galaxy cores with the smallest values and quasar cores with the highest values. In spite of all these limitations, the values derived give an idea of the typical values of these parameters (and their range). We emphasize that the derived values are only order of magnitude estimates. We also emphasize the fact that this method provides size estimates for galaxy cores which are ~100 times smaller than the telescope resolution; this, in turn, improves the other estimates by several orders of magnitude!

The values obtained here for the CD quasars are similar to those obtained from detailed modelling of well-studied individual sources (for e.g. Bregman et al. 1986). The parsec-scale sizes we derive for the cores here are similar to the 0.5-pc sizes estimated from variability data (Valtaoja & Terasranta 1993). Recent VLBI studies at mm wavelengths with a few tens of μarcsec angular resolutions have revealed that the cores of blazars have

Table 4. Spectral parameters (observed) of the cores of radio sources.

Source	z	$\nu_{\rm ssa}$ GHz	$\alpha_{>\rm ssa}$	$S_{\rm ssa}$ mJy	S_{1G} Jy
HRRG	2.5	5	0.75	2.5	0.005
HRCDQ	1.0	50	0.75	4000	75
LRCDQ	0.5	50	0.65	5000	150
LDQs					
0410+110	0.306	10	0.72	225	1.52
0704+384	0.579	15	0.97	65	1.36
0836+195	1.691	20	1.26	50	2.39
0837-120	0.200	13	0.56	200	1.16
1100+772	0.311	15	1.21	80	3.06
1830+285	0.594	35	0.84	900	13.9

Notes: The source categories are high-redshift radio galaxies from our sample (HRRG), high- and low-redshift core-dominated quasars from Gear et al. (1994) (HRCDQ and LRCDQ) and lobe-dominated quasars (LDQ) from Antonucci et al. (1990) and Gopal-Krishna & Steppe (1990). The columns shown are redshift, synchrotron self-absorption turnover frequency, spectral index of the optically thin emission at $\nu > \nu_{\rm ssa}$, flux density at $\nu_{\rm ssa}$ and the flux density of the core at 1 GHz extrapolated from the spectrum at $\nu > \nu_{\rm ssa}$.

Table 5. Derived parameters of the cores of radio sources in the plasma rest frame. The linear size (L) is in parsec, the magnetic field (B) in gauss and the electron number density ($n_{\rm e}$) in particle cm^{-3}. θ is the angle between the relativistic jet and the line of sight. The parameters have been calculated for Lorentz factor $\gamma = 5$ and 10.

Source	$\theta°$	L	B ($\gamma = 5$)	$n_{\rm e}$	L	B ($\gamma = 10$)	$n_{\rm e}$
HRRG	55	1.1	0.7	460	1.9	0.9	960
HRCDQ	8	0.4	0.9	820	0.4	0.9	810
LRCDQ	8	0.3	0.9	620	0.3	0.9	610
HRRG	65	1.4	0.8	630	2.3	1.1	1300
HRCDQ	12	0.5	1.0	1200	0.6	1.1	1600
LRCDQ	12	0.4	1.0	900	0.5	1.2	1200
LDQs							
0410+110	40	1.2	0.6	230	1.8	0.7	470
0704+384	25	0.4	0.8	1300	0.7	1.0	2300
0836+195	15	0.3	1.1	7800	0.4	1.2	11000
0837-120	25	0.3	0.5	120	0.5	0.7	240
1100+772	40	0.7	1.1	7200	1.3	1.4	13000
1830+285	15	0.3	0.9	1000	0.4	1.0	1500

considerably smaller sizes of $\sim 10^{17}$cm (Baath et al. 1992). The difference of a factor of 30 between these direct measurements of the angular size and those deduced from the SSA model could be because of several reasons; these sources were selected for their large fluxes at 100 GHz and hence their SSA turnover is probably at frequencies higher than the typical value of 50–100 GHz deduced for the Gear et al. (1994) sample. Further, inhomogeneous source models of SSA (Condon & Dressel 1973) show that emission at frequencies around and above the turnover arises from the very central regions (often the inner fifth or smaller) of the source.

The radio galaxies and quasars studied here have similar core parameters, which argues for similar physical processes and conditions in their cores. The quality of the data is insufficient to address the much stronger point raised by unification schemes – that galaxies and quasars are intrinsically similar objects viewed from different angles. Well-determined spectra and accurate Doppler factors are essential for testing specific unification schemes using this phenomenon. We also note that unification schemes should be tested within well-defined flux-limited radio samples selected on the basis of extended emission. The three samples here (CDQs, LDQs and radio galaxies) do not satisfy the conditions; they simply happen to be the only sources in which the SSA turnover has been observed.

Given the observational constraints imposed by the sensitivity and resolution of telescopes, CD quasars offer the best hope for studying the cores of radio sources directly, at least in the near future; we may not be erring too much in applying our knowledge of cores of CD quasars to radio galaxies and extended quasars as well. However, as we have outlined, the study of the weak radio cores in the region where they steepen beyond the SSA turnover circumvents the observational constraints and can be used to estimate the physical parameters.

3.3 CD quasars and BL Lac objects

Gear et al. (1994) have also presented core flux densities of the cores of a sample of 22 BL Lacs. We have carried out a similar analysis of the crf spectral index distribution for BL Lacs as described before for CDQs. The distribution for the entire sample of BL Lacs is plotted in Fig. 2(a) while the high- and low-redshift BL Lacs (division at $z = 0.3$) have been compared in Fig. 2(c). Table 3 lists the mean spectral index of BL Lacs at frequencies above the turnover.

BL Lac objects also show a change from flat to steeper spectra; however the change is smaller and the spectra are only marginally steeper than the canonical value of $\alpha = 0.5$. The two redshift classes appear to have very different mean spectral indices (see Table 3) but a closer examination shows that all the difference is due to the 193-GHz data where the low-redshift sources predominate and the spectrum is still in the process of steepening. The mean for the two highest frequencies shows no difference between the high- and low-redshift sources.

Discussing the radio–submm spectral index distribution of the blazars in their sample, Gear et al. (1994) considered the possibility that the difference between BL Lacs and CDQs may be due to differences in their redshift distribution and/or viewing angles of the jets. Though they could not reject these two possibilities using their data, they argued for intrinsic differences between the two classes. However, re-analysing their data using rest-frame spectral indices and different redshift intervals, it is clear that the difference is not due to their redshift distributions (Fig. 2 and Table 3). BL Lacs only show a tendency to steepen towards higher frequencies. The spectral index is still around 0.5 – just marginally into the 'steep' regime – even at the highest frequencies. Over the same frequency range, quasars show a definite steepening to a spectral index of about 0.7. The rest-frame spectra of QSRs and BL Lacs at $z < 0.7$ are very different indicating that the cores of BL Lacs and quasars are intrinsically different though they have several properties in common.

It has been suggested that BL Lacs are the beamed counterparts of FR I radio galaxies along the lines of the quasar–FR II radio galaxy unification scheme. It is well known that the extended emission has a flatter spectral index in FR I sources compared to that in FR II sources. It needs to be examined whether a single explanation can account for the flatter spectra of both the cores and the extended emission in BL Lac/FR I sources *vis-à-vis* the quasar/FR II group.

3.4 Electron spectrum

The steep spectra of CDQs at frequencies >200 GHz (crf) show no evidence of further steepening towards higher frequencies (Fig. 2). However the frequency range is not very large and the result may not be very significant given the spread in the values. The value of the core spectral index above the turnover for CDQs is similar to that seen in the lobes of extended radio sources at a few 100 MHz. This low-frequency spectral index, where electrons have not had time to radiate their energy, should correspond to the spectrum of the electron energy at the time of injection. It is surprising that the spectrum does not steepen very rapidly in the cores at the very high frequencies under discussion (the synchrotron half-life for emission at 200 GHz in a 1-G field is less than a month). However, under conditions of continuous injection of electrons together with expansion losses dominating over synchrotron losses, the electron spectrum remains unchanged (Pacholczyk 1970; Moffet 1975). This may well be the case in these compact cores with high internal energy density.

The high-redshift CDQs from the sample of Gear et al. (1994) have a steeper spectral index than their low-redshift counterparts (Fig. 3). Numerical simulations have shown that under conditions of strong relativistic shock, an increase in the Lorentz factor γ results in the generation of a steeper electron energy spectrum (Ballard & Heavens 1992). This would lead to a luminosity–spectral index correlation in Doppler-boosted core dominated sources and hence a redshift–spectral index correlation in a flux-limited sample as has been observed here. This should also result in a correlation between the observed superluminal velocity and redshift. The data presented in Vermeulen & Cohen (1994) for core-flux selected sources do show some increase in superluminal velocity with redshift although the correlation is marginal and dependent on the value of Ω_0 used.

4 CONCLUSIONS

The spectra of radio cores in high-redshift galaxies appear to steepen at 15–30 GHz in the cosmological rest-frame (crf). Both LDQs and CDQs have been reported to show a similar steepening, although at considerably higher frequencies. We show that the observations are consistent with the cores of galaxies and quasars being intrinsically similar in the rest frame of the emitting plasma (prf). The difference in the crf could be a result of differential Doppler shifting in the two classes as a result of relativistic aberration. Based on these observations we suggest that the spectra of cores in radio sources are flat below ~20 GHz in the prf (i.e. ~4 GHz in the crf for galaxies on account of the redshift due to

relativistic motion in the core) and steepen to a spectral index of 0.7 towards higher frequencies.

This model can be confirmed by high-resolution observations of radio galaxy cores between 1 and 20 GHz in the crf. The spectra of cores must be examined for gradual but systematic steepening between 5 and 20 GHz. Previous studies of galaxies up to 10–15 GHz have not reported steep-spectrum cores. It is likely that this effect is present in extant data. It may not have been noticed due to many reasons – the values may still lie within the '$\alpha = 0.5$ barrier' and may have been dismissed earlier as either aberrations or errors because of the faintness of the cores.

Several physical parameters of the cores have been calculated from the observed spectra using the theory of synchrotron self-absorption. We derive similar values for the physical size ($\sim$1 pc), magnetic field (1 G) and electron number density (1000 cm^{-3}) for both quasar and galaxy cores. The similar values argue for similar physical processes and conditions in the cores of galaxies and quasars.

We emphasize that the core sizes derived for galaxies in this study are more than 100 times smaller than the telescope resolution. The turnover in the spectra is a useful tool for probing the faint cores of galaxies which are usually too faint for VLBI studies.

We also find evidence for some differences in the spectra of CD quasars and BL Lacs. The turnover is more pronounced and the magnitude of the steepening larger in the case of CDQs. Further, higher redshift CDQs have steeper spectra than their lower redshift counterparts. This is likely to be a secondary correlation arising from a spectral index–Lorentz γ (and hence luminosity of Doppler-boosted core-dominated sources) correlation.

ACKNOWLEDGMENTS

We would like to thank Dr Chris Carilli for calibrating some of the high-resolution VLA observations of the galaxies in our sample. The VLA is operated by the Associated Universities, Inc., under co-operative agreement with the National Science Foundation.

REFERENCES

Antonucci R., Barvainis R., Alloin D., 1990, ApJ, 353, 416
Athreya R. M., 1996, PhD thesis, Univ. of Bombay
Baars J. W. M., Genzel R., Pauliny-Toth I. I. K., Witzel A., 1977, A&A, 61, 99
Baath L. B. et al., 1992, A&A, 257, 31
Ballard K. R., Heavens A. F., 1992, MNRAS, 259, 89
Barthel P. D., 1989, ApJ, 336, 606
Barthel P. D., Schilizzi R. T., Miley G. K., Jagers W. J., Strom R. G., 1985, A&A, 148, 243
Bregman J. N., 1990, A&AR, 2, 125
Bregman J. N. et al., 1986, ApJ, 301, 708
Bridle A. H., Fomalont E. B., 1978, AJ, 83, 704
Bridle A. H., Fomalont E. B., Cornwell T. J., 1981, AJ, 86, 1294
Brown L. M. J. et al., 1989, ApJ, 340, 129
Carilli C. L., 1995, A&A, 298, 77
Carilli C. L., Owen F. N., Harris D. E., 1994, AJ, 107, 480
Condon J. J., Dressel L. L., 1973, Astrophys. Lett., 15, 203
Cotton W. D. et al., 1980, ApJ, 238, L123
Gear W. K. et al., 1994, MNRAS, 267, 167
Gopal-Krishna, Steppe H., 1990, in Miller H. R., Wiita P. J., eds, Proc. Georgia State Univ. Conf. on Variability of AGN. Cambridge Univ. Press, Cambridge, p.194
Impey C. D., Neugebauer G., 1988, AJ, 95, 307
Jones T. W., Rudnick L., Owen F. N., Puschell J. J., Ennis D. J., Werner M. W., 1981, ApJ, 243, 97
Kellermann K. I., Pauliny-Toth I. I. K., 1969, ApJ, 155, L71
Kellermann K. I., Pauliny-Toth I. I. K., 1981, ARA&A, 19, 373
Knapp G. R., Bies W. E., van Gorkom J. H., 1990, AJ, 99, 476
Lonsdale C. J., Barthel P. D., Miley G. K., 1993, ApJS, 87, 63
McCarthy P. J., Kapahi V. K., van Breugel W., Subrahmanya C. R., 1991, AJ, 102, 522
McCarthy P. J., Kapahi V. K., van Breugel W., Athreya R. M., Persson S. E., Subrahmanya C. R., 1996, ApJS, in press
Miley G. K., 1980, ARA&A, 18, 165
Moffet A. T., 1975, in Sandage A., Sandage M., Kristian J., eds, Stars and Stellar Systems IX, Galaxies and the Universe. Univ. of Chicago Press, Chicago, p.211
Pacholczyk A. G., 1970, Radio Astrophysics. W. H. Freeman & Co., San Francisco
Saikia D. J., Kulkarni V. K., Porcas R. W., 1986, MNRAS, 219, 719
Sanders D. B., Phinney E. S., Neugebauer G., Soifer B. T., Matthews K., 1989, ApJ, 347, 29
Valtaoja E., Terasranta H., 1993, in Davis R. J., Booth R. S., eds, Proc. NRAL Conf., Sub-Arcsecond Radio Astronomy. Cambridge Univ. Press, Cambridge, p.167
Vermeulen R. C., Cohen M. C., 1994, ApJ, 430, 467

APPENDIX A: INTRINSIC SOURCE PARAMETERS IN THE PLASMA REST-FRAME FROM OBSERVED SPECTRA

From the theory of synchrotron self-absorption, the turnover frequency is given by

$$\nu_{\rm ssa} = \left(\frac{f_\eta\, S_{\rm ssa}^{2/5}\, B^{1/5}}{\Theta^{4/5}}\right)\left(\frac{1+z}{\Gamma}\right)^{(1+2\alpha)/5}. \qquad \text{(A1)}$$

See below for the key to the symbols.

(The relativistic and cosmological factors have been derived using the relation given by Moffet (1975) for a stationary source in Euclidean geometry.) The magnetic field is the only parameter that is not directly observable. Fortunately, the fifth root of the magnetic field being the relevant quantity, even an error of an order of magnitude in B would introduce only an error of 1.6 in the $\nu_{\rm ssa}$. The usual estimate used for the magnetic field is obtained by applying the minimum energy condition (approximately equivalent to equipartition of the energy between the magnetic field and the relativistic particles). In terms of the observables this equipartition field is given by

$$B = (0.076\, h^{2/7})\left(\frac{S_{\rm 1G}^{2/7}}{\Theta^{6/7}}\right)\left[\frac{(1+z)^{(9+2\alpha)/7}}{(\sqrt{1+z}-1)^{2/7}}\right]\left[\frac{1}{\Gamma^{(6+2\alpha)/7}}\right] \qquad \text{(A2)}$$

for $0.5 < \alpha < 1.1$ (accurate to within 15 per cent at the extreme values). Combining equations (A1) and (A2), one can eliminate the magnetic field to obtain

$$\nu_{\rm ssa} = (0.60\, f_\eta\, h^{2/35})\left(\frac{S_{\rm ssa}^{2/5}\, S^{2/35}}{\Theta^{4/5}}\right) \times \left[\frac{(1+z)^{(16/35)(1+\alpha)}}{(\sqrt{1+z}-1)^{2/35}}\right]\left[\frac{1}{\Gamma^{(13+16\alpha)/35}}\right], \qquad \text{(A3)}$$

from which the size of the unresolved core can be estimated. Using this, one can also estimate the equipartition magnetic field. These parameters can be used to estimate the number density of electrons in these cores using the relationship

$$n_{\rm e} = (2.4\ 10^{-3}\ g_\alpha\ h)\left(\frac{S_{\rm 1G}\, B}{\Theta^3}\right)\left(\frac{(1+z)^{(9+2\alpha)/2}}{(\sqrt{1+z}-1)}\right) \times \left(\frac{1}{\Gamma^{(3+\alpha)}}\right). \qquad \text{(A4)}$$

Key to the symbols

α: spectral index ($S \propto \nu^{-\alpha}$) in the optically thin region of the spectrum.

B: magnetic field in gauss.

f_η: a function of electron energy distribution index $\eta[n(E) \propto E^{-\eta}]$; $(\eta, f_\eta) \equiv$ (1.5, 6.0), (2.0, 7.0), (2.5, 8.0), (3.0, 8.7).

g_α: the function $(1/\nu_1)^{\alpha}[\frac{1-(\nu_1/\nu_2)^{\alpha}}{\alpha}]$; ν_1 and ν_2 are the critical frequencies, in GHz, corresponding to the lower and upper cut-offs in the electron energy distribution.

Γ: Doppler factor $\equiv[\gamma\,(1-\beta\cos\theta)]^{-1}$, where Θ is the angle between the line of sight and the relativistic jet and γ and β pertain to the jet velocity.

h: Hubble's constant in units of 100 $\mathrm{km\,s^{-1}\,Mpc^{-1}}$. The density parameter used is $\Omega_0 = 1$.

n_e: total electron density in $\mathrm{cm^{-3}}$.

ν_{ssa}: synchrotron self-absorption turnover frequency in GHz.

S_{ssa}: flux density at ν_{ssa} in Jy.

$S_{1\,GHz}$: flux density at 1 GHz, extrapolated from the optically thin region of the spectrum.

Θ: angular size of the component in milliarcsec.

z: cosmological redshift.

This paper has been typeset from a TEX/LATEX file prepared by the author.